Journal Of Environmental Chemical Engineering
March 2015, Volume 3 Issue 1 Pages 210-216
https://doi.org/10.1016/j.jece.2014.09.021
https://archimer.ifremer.fr/doc/00266/37739/

Characterization of exopolysaccharides after sorption of silver ions in aqueous solution

Deschatre Marine [1, 2, 3, 4], Lescop B. [5], Simon Colin Christelle [2, 3, 4], Ghillebaert F. [6], Guezennec Jean [7], Rioual S. [5, *]

[1] Mexel Ind SAS, F-60410 Verberie, France.
[2] Inst Francais Rech Exploitat Mer, Ctr Brest, UMR 6197, Lab Microbiol Environm Extremes, Plouzane, France.
[3] Univ Bretagne Occidentale, UEB, IUEM, Lab Microbiol Environm Extremes,UMR 6197, Plouzane, France.
[4] CNRS, UMR 6197, Lab Microbiol Environm Extremes, Plouzane, France.
[5] Univ Brest, Lab Magnetisme Bretagne, EA 4522, 6 Ave Gorgeu, F-29285 Brest, France.
[6] Ecotox, F-62380 Affringues, France.
[7] AiMB, F-29280 Plouzane, France.

* Corresponding author : S. Rioual, email address : rioual@univ-brest.fr

Abstract :

Biosorption of silver ions by several exopolysaccharides (EPS) differing from each other in their chemical composition and functional groups was investigated. EPS were characterized before and after Ag(I) biosorption by comprehensively using X-ray photoelectron spectroscopy (XPS), Fourier transform infrared spectroscopy (FTIR), X-ray diffraction, transmission electron microscopy (TEM). The role of the different functional groups in the biosorption process was observed. In particular, sulfate groups were seen playing a major role. XPS and FTIR methods showed that the composition of lowest efficient EPS changed after Ag(I) biosorption with a relative increase of the carboxylate ions content. This change was accompanied by the formation of mainly silver oxide nanoparticles. As the consequence, the reducing character of the EPS is expected to influence the silver sorption capability of the EPS.

Graphical abstract

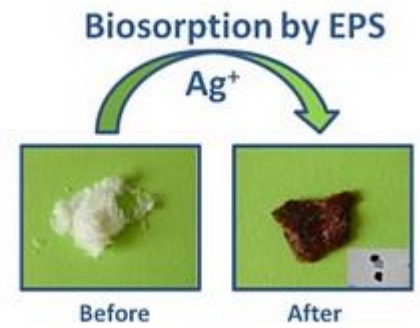

Highlights

► Ag^+ biosorption by four EPS differing from each other in their chemical composition. ► XPS, FTIR, XRD, TEM were applied to characterize the EPS before and after sorption. ► The role of sulphate groups in the biosorption is highlighted. ► Silver and silver oxide nanoparticles were observed.

Keywords : Exo-polysaccharide, Silver ions, Biosorption, XPS analysis

1. Introduction

During the last decades, silver ions were extensively used in many industrial activities such as in electronics, jewellery, photography or electroplating domains, resulting in increasing contamination of waste water, especially in aquatic environment [1]. Actually silver is one of the most toxic metal, in particular in its ionic form [2,3,4] and its absorption by humans can cause severe dysfunction of kidney, reproduction system, liver, brain and central nervous systems. Considering the serious environmental problems and the damage to human health caused by this toxic metal, great attention has been paid in its removal from water. Furthermore, recovery of silver is of economic interest due to its high commercial value. Different methods do exist to recover metal ions including conventional ones such as electrolysis [5], precipitation [6], flotation [7], ion-exchange [8] or adsorption [9,10]. Among these methods, biosorption of silver ions by biomaterials is becoming an emerging technique due to its simplicity, low cost and efficiency. Recently, a number of biosorbents were developed and tested for removal and recovery of Ag^{+}, such as fungi *Cladosporium cladosporides 1* [11], bacteria *Myxococcus xanthus* [12], persimmon tannin [13] or chitosan resin [10].

Bacterial exopolysaccharides (EPS) are high molecular weight polymers excreted by numerous bacteria into the surrounding environment, and are considered as promising biosorbents because of their diversity of structures and properties along with the ease of production and biodegradability. Actually, EPS present ionisable functional groups such as carboxyl, acetate, hydroxyl, amine, phosphate or sulfate groups which may act as active sites for ionic biosorption [14]. They have been successfully used in the past for heavy metal ions removal from aqueous solutions [15-18]. However, only recently, Deschatre *et al*. [19] focused on sorption of silver ions by EPS. In this study, authors investigated sorption capacity of four EPS differing from each other in their chemical composition, and compared their efficiency for silver

and copper ions capture. Metal biosorption experiments were conducted in batch process and showed the influence of factors such as initial metal concentration, EPS concentration or pH, on the retention capacity. Maximal metal sorption capacities were 333 mg Ag/g EPS M3 and 400 mg Cu/g EPS M1, thus highlighting differences in the selectivity of each EPS. Such selectivity could be explained, at least partially, by the nature of functional groups within each EPS, as suggested by Fourier Transform Infrared Spectroscopy (FTIR) analyses performed on EPS before and after metal sorption. However, mechanisms involved in the sorption mechanism of silver remain unclear. The aim of the present study was to identify EPS functional groups involved in silver sorption to better understand sorption mechanisms to predict and improve silver ions recovery. Thus, chemical structure of four EPS was studied before and after silver sorption, using X-ray Photoelectrons (XPS), X-ray diffraction (XRD), FTIR and Transmission Electron Microscope (TEM). Only the use of such complementary techniques enables one to get a good understanding of the sorption mechanism.

2. Material and methods

Chemicals

All chemicals used in this study were of analytical grade. Stock solutions of Ag(I) (500 mg. L^{-1}) was prepared by dissolving ($AgNO_3$) from Sigma Aldrich in ultrapure water. Bacterial production of exopolysaccharides along with the associated extraction and purification protocols have been previously described [20].

Metal biosorption experiments

Biosorption experiments were performed in a flask by dissolving 50 mg of dry EPS in 100 ml of silver solution at initial concentration of 500 mg.L^{-1}. Experiments were performed in the

dark due to the photosensitivity of silver nitrate. Solutions were prepared in triplicate and were gently shaken during 3 hours. During experiments, pH was regularly checked. At the end of the experiment, solutions were ultrafiltered using Pellicon Tangential Flow Filtration Cassettes with a nominal molecular weight cutoff of 100 kDa to eliminate all free silver ions remaining in the solution. Permeates were analyzed by inductive coupled plasma atomic emission spectroscopy (ICP AES; Horiba Jobin Yvon ULTIMA 2) to determine silver ions concentration, while retentates were freeze-dried prior to further analyses by XRD, XPS FTIR and TEM.

Analytical techniques

Crystalline structure of four EPS (M1, M2, M3, M4) was analysed by X-ray diffraction (XRD) with an Empyrean Panalytical apparatus using the CuKα radiation. Composition of EPS polymers was determined by X-Ray photoelectron spectroscopy (XPS) before and after sorption. Briefly, the experimental apparatus consisted of an Mg-Kα X-ray source (Thermo VG) and a cylindrical mirror analyser from RIBER. The fitting procedure was made by CasaXPS software and by considering linear and Shirley backgrounds [21]. FTIR spectra of dried EPS were recorded on Thermo Scientific Nicolet iS10 FTIR spectrometer, equipped with a universal attenuated total reflectance sampling device containing diamond Zn/Se crystal. Spectra were scanned at room temperature in transmission mode over the wave number range of 4,000-600 cm^{-1}, with a resolution of 4 cm^{-1}. The TEM microscope used for the observation of silver nanoparticles created by precipitation was a JEOL JEM 1400.

3. Results and discussion

3.1 X-Ray Photoelectron spectroscopy

It is well admitted that biosorption of metals ions by biosorbents is due to the presence of ionisable functional groups such as carboxyl, acetate, hydroxyl, amine, phosphate, and sulfate groups [14], which are considered as potential binding sites for metal ions sequestration [22]. Metal biosorption occurs by interactions between metallic cations and EPS functional groups through complex mechanisms such as ion exchange, precipitation, adsorption or complexation [22]. To investigate the influence of functional groups involved in silver biosorption mechanism by EPS, XPS analyses were carried out on EPS before and after silver biosorption experiment. As shown by Table 1, neutral sugars and uronic acids appeared in the four studied EPS. XPS C(1s) and O(1s) spectra were thus systematically recorded. One should note that EPS M2 differs from other EPS since it is mainly composed of neutral sugar and shows a high polydispersity index (Ip=4.2) and a relatively low (870 kDa) molecular mass [19]. Since EPS M1 and EPS M4 contain sulfate and hexosamine content, respectively, N(1s) and S(2p) spectra are also considered in the following.

3.1.a. XPS characterization of EPS before biosorption

C(1s) spectra presented in figure 1(a) displays an important structure at 284.8 eV due to the presence of C-C and C-H bonds and an asymmetric tails at high binding energy due to the presence of carbon based functional groups. Generally, observed feature can be reproduced by considering the four possible C_i (i=0,1,2,3) contributions indicated by arrows in Fig. 1(a) which corresponds to non-functionalized carbon (C-C, C-H), carbon singly bounded (i.e. C-O or C-N for M4), carbon doubly bounded to oxygen (i.e. acetal carbon O-C-O or C=O) and carbon bounds to two oxygens (O=C-O). The relative energies of the three last contributions with respect to the first one are 1.7±0.1, 3.1±0.1 and 4.4±0.2 eV [23,24], respectively. To decompose the spectra, only the three first components (C_i, i=0, 1, and 2) were considered here due to the weakness of

the fourth component. The binding energies and intensities of these components derived from the fitting procedure are given in Table 2. As observed, the binding energy of C_1 is very close to the predicted value of 286.5 eV and indicates the presence of alcohol groups C-OH for EPS M1, M2, M3 and M4 and C-N for EPS M4. In contrast, the C_2 contribution is clearly shifted toward high energy with respect to the expected nominal value of 287.9 eV. This reveals the importance of carboxylate ions which lead to contribution at 288.3 eV [25]. However, O-C-O or C=O bonds may also be present, in agreement with the expected structure of polysaccharides. Table 2 displays the total intensity of the carbon based functional groups (C_1+C_2) and the C_1/C_2 ratio for each EPS. It appears then clearly that there is an important difference in the total quantities of available functional groups in the four EPS. Furthermore, the ratio between the amount of carboxylate and alcohol groups differs in the EPS leading to a relative enrichment of alcohol for EPS M2 and carboxylate for EPS M4.

The O(1s) spectra are presented in Fig. 1(b). Spectra were deconvoluted by considering only one contribution. Positions and intensities of this contribution are reported in Table 2. By comparing the intensities of the O(1s) peaks with the total amount of the C_1+C_2 functional groups discussed above, a very good agreement is found except for M_1. This evidences that the carbon based functional groups dominates for EPS M2, M3 and M4 while the contribution of sulfate groups needs to be considered for EPS M1. The chemical nature of this EPS and probably its biosorption capability has thus to be discussed separately. For EPS M2, M3, and M4, the O(1s) peaks display different binding energies. This behaviour is explained by the composition of the EPS already noticed in the analysis of the C(1s) spectra. Indeed, M2 and M3 display peaks localized at high binding energies due to similar composition with high content of OH groups and lower content of carboxylate ions. For EPS M4, the importance of carboxylate leads to a decrease of the binding energy. For EPS M1, as stated above, the O(1s) spectra is more complex due to the

presence of hydroxyl, carboxylate and sulfate groups. The N(1s) and S(2p) spectra were measured before and after silver uptake for EPS M4 and M1, respectively (Fig 1. from supporting material). For EPS M4, the N(1s) line is localized at 399.7 eV, a value attributable to amine groups [26]. For EPS M1, before absorption, the S(2p) peak observed at 169 eV is explained by the sulfate groups.

The presented results allow a clear identification of the active functional groups in the EPS before sorption. They are in fully agreement with the expected composition of the EPS. Indeed, they show i) for EPS M1, the presence of alcohol, carboxylate and sulfates groups, ii) for EPS M2, the high contribution of alcohol groups with negligible amount of carboxylate groups, iii) for EPS M3, an increase of the amount of carboxylate groups compared with EPS M2 due to a higher content of uronic acid, and finally iv) for EPS M4, an enhancement of the carboxylate quantities and the presence of amine groups. We note, however, that the main constituent of functional groups is the alcohol one. From these results, it appears also clearly that the availability of total functional groups including sulfate increases from EPS M4 to M3. This order does not correspond to the ranking in order of silver uptake capability observed by Deschatre *et al*. [19], showing either the selectivity of functional groups in sorption or different processes which may takes place.

3.1.b. XPS characterization of EPS after biosorption

In table 3, we present the results achieved after the decomposition of the C(1s) and O(1s) spectra after biosorption. Spectra are presented in the supporting material part. The positions of the C_1 and C_2 contributions derived from the fitting procedure remain almost identical to those observed before biosorption. For EPS M2, M3 and M4, the amount of total carbon based functional groups (C_1+C_2) is reduced by almost the same ratio. However, by considering the

change of the C_1/C_2 ratio, it appears that biosorption by EPS M3 is characterized by a similar decrease of intensities of both C_1 and C_2 functional groups. In contrast, for EPS M2 and M4, an important decrease of the C_1 intensity with respect to C_2 is found. This result demonstrates that some of the EPS are subjected to a change on their chemical structure during the biosorption and highlights that different sorption mechanisms are expected to occur in EPS M3 with respect to EPS M2 and M4. EPS M1 differs from the others by the presence of sulfates. For this EPS, the biosorption is correlated to a stronger decrease of the total amount of the carbon based functional groups. As observed for EPS M3, the same decrease of the intensities of C_1 and C_2 is observed for EPS M2.

Table 3 displays also the results of the fitting procedure applied to the O(1s) spectra. For EPS M2, M3 and M4, as seen in the table, the total intensity of the O(1s) peak is decreasing by almost the same factor as the one found by the fitting procedure applied on the C(1s) spectra. This is fully explained by the fact that hydroxyl as well as carboxylate groups are contributing equally to both spectra. For EPS M1, the O(1s) intensity also decreased but its intensity remained higher than these results given by the C(1s) contribution due to the influence of sulfates which are observed in the O(1s) but not in the C(1s) spectra, respectively.

In figure 2, we present Ag(3d) spectra after silver biosorption by the four EPS. Spectra were fitted using a linear background and two contributions associated to the two $Ag(3d_{3/2})$ and $Ag(3d_{5/2})$ components. Results of the fitting are presented in Table 4. The binding energies of the $Ag(3d_{5/2})$ photolines are well above 368.2 eV, the typical value of metallic silver. As discussed by Shin *et al.* [27], such shifts may be attributed to different particle sizes, crystal structures, or chemical bondings of the metallic silver particles. We note that the observed energies are very close also to that found for silver nanoparticules with size of about 7 nm protected by carboxylate ions [28] or decanoate [29]. Due to this supplementary shift, the interpretation of Ag(3d) spectra

is not an easy task and an interpretation of the data including the evaluation of the modified Auger parameter α is highly desirable. This parameter which is equal to the sum of the kinetic energy of an Auger line and the binding energy of the associated photoelectron line provide additional chemical information on the species since it is independent of additional shifts created for example by charged sample. For that, we measured the $M_4N_{45}N_{45}$ Auger peak spectrum for the EPS M3 which presented the higher silver content. Auger parameter was equal to 724.5 eV. For comparison, it was found to be 726.3 and 724.5eV in bulk silver and pure Ag_2O, respectively; indicating here the presence of Ag^+ [30]. Presence of silver oxide is not possible here due to their lower energies than 368 eV and to the non-observation of the O(1s) contribution near 530 eV. From these results, for EPS M2, M3 and M4, we expect thus that silver is present in the EPS in the form of Ag^+ ions surrounded mainly by hydroxyl and carboxylate bonds. This result is in agreement with several studies made on the biosorption of metals [11,31]. In the literature, it is indeed frequently proposed that metal ions carboxylate complexes of different types are formed such as anionic or uncoordinated form, via unidentate coordination, via bidentate chelating coordination or via bidentate bridging coordination [32]. To explain the interaction between silver ions and hydroxyl groups, we expect that weak intra-molecular hydrogen bonding with hydroxyl groups may play a significant role. For EPS M1, as discussed above, the amount of sulfate groups is not negligible compared to hydroxyl and carboxylate functional groups. In this case, Ag^+ ions should then be stabilized in the EPS throughout interactions between these three groups. This scenario is fully validated by the S(2p) sulfate peak (supporting material) which displays a shift in energy after silver biosorption toward high energy, indicating the bonding between Ag^+ and sulfate groups. For EPS M4, after biosorption, no difference was observed in the N(1s) spectrum, leading to the conclusion that nitrogen is not

active during the process.

In table 4, the intensity of Ag(3d) peak is representative of the amount of silver biosorbed by the EPS. The ranking EPS in order of silver uptake capability is thus the following: EPS M3(1), M1(0.55), M4(0.48) and M2(0.29), in agreement with the determination of silver concentration made by ICP AES [19]. As stated above, such order is not correlated to the ranking of the amount of total functional groups available before biosorption indicating different efficiencies of the hydroxyl, carboxylate and sulfate functional groups. The low efficiency of the EPS M2 may indicate thus that hydroxyl groups which are in majority in this EPS are not efficient with respect to carboxylate groups. However, this consideration does not explain the important difference in sorption capability observed between EPS M3 and EPS M4, this latter being enriched in carboxylate ions. The change of the polymer composition observed on EPS M2 and M4 after sorption remain also unclear and should affect the sorption capabilities.

3.2 FTIR

To further investigate the role of EPS functional groups during sorption, FTIR spectra of EPS before and after biosorption are given in figure 3. FTIR spectra of native EPS showed an intense band in the 1200/1000 cm^{-1} region that can be assigned to ring vibrations overlapping with stretching vibrations of (C-OH) side groups and the (C-O-C) glycosidic bond vibration. As shown by M. Kacurakova *et al.* [33], positions of the observed maxima are explained by the backbone of the polysaccharide and by the chain constituents. Relative positions of axial and equatorial OH groups also influence positions of main peaks. For all EPS, bands attributable to symmetric stretching vibration near 1400 cm^{-1} and asymmetric stretching band at about 1600 cm^{-1} of carboxylate ions are observed [32]. EPS M1 displays additional doublet at about 1250 cm^{-1} attributed to the presence of sulfates.

As seen in the figure 3, composition of EPS M1 and M3 remains almost identical before and after biosorption. In contrast, for EPS M2 and M4, a strong increase of the intensity of the asymmetric carboxylate line is clearly observed. Such behaviour is in very good agreement with the results obtained by the XPS measurements and demonstrates that different mechanisms occur during biosorption by these EPS. The increase of the carboxylate contribution is definitely higher in the FTIR spectra than in XPS. This difference may be explained by the different regions in depth probed by the two techniques and also reveals the heterogeneity of the polymer under investigation.

3.3 X-Ray Diffraction characterization and Transmission Electron Microscopy analysis

Additional information on the status of silver ions trapped onto the EPS was obtained by X-Ray diffraction analyses. Before exposition, no pattern was reported due to the non-crystallinity of the EPS. Figure 4 shows XRD patterns of EPS M1, M2, M3 M4 after Ag biosorption. XRD pattern of EPS M1 is very different from the others and displays numerous lines attributed to Ag_2SO_4. As stated above, this finding highlights the particular behaviour of EPS M1 due to the presence of sulfate groups. XRD patterns of EPS M2, M3 and M4 are very close and show the presence of Ag, Ag_3O_4 and Ag_2O nanoparticles in the EPS. This result is in agreement with a recent study on the Ag^+ biosorption by *Saccharomyces cerevisiae* cell walls [34] which proposes the formation of micro-precipitates as a possible mechanism for biosorption. In figure 4, EPS M3 is highly dominated by metallic Ag particles compared to EPS M2 and M4. Indeed, the five major peaks are indexed as face-centered cubic (fcc) structure [35] and indicate a polycrystalline structure of metallic silver with an intense (111) preferred orientation. Dimension of crystallites can be estimated to about 10 nm according to Scherrer's formula (see supporting material). Additional peaks are also observed at positions corresponding to Ag_2O and Ag_3O_4 [36]

with crystallites sizes of about 15 nm. Data of both EPS M2 and M4 shows the same peaks with however variations of relative ratios. Peaks assigned to silver oxides are indeed more intense than those of metallic Ag. The achieved XRD results allowed us to conclude that silver biosorption process is a complex phenomenon in which formation of oxide and metal nanoparticles must be taken into account because it directly affects silver ions availability and thus sorption potential. Moreover, our results demonstrate that biosorption mechanism is different in EPS M2 and M4 with respect to M3, leading to the formation of either a majority of oxide or metallic nanoparticles. This difference should also be correlated to the FTIR and XPS results discussed previously where an increase of the carboxylate contents is observed for EPS M2 and M4 with respect to M3.

The presence of metallic silver nanoparticles can be explained by reduction of silver ions into metallic silver. Such process is a well known method to produce silver metallic nanoparticles and it was recently shown that chemical reducing agents can be replaced by molecules produced by living organisms such as bacteria, fungi, algae or plants [37,38]. In the present study, we evidenced that bacterial EPS can also enable reduction of silver ions and can be thus considered as potential candidates for elaboration of metallic silver particles. As proposed by Lin *et al.*, oxidation of hydroxyl to carboxyl group may explain the presence of metallic silver [31]. In this case, reduction of silver is accompanied by the release of H^+ ion in the solution leading to a reduction of pH [31,39]. We note that such pH variation was also observed by Deschatre *et al.* [19]. However, this scenario does not explain the formation of silver oxide nanoparticles observed by XRD measurements. As proposed by Nersisyan et *al.* [40] on glucose, Ag_2O can first be created by the reaction between OH^- and silver ions in solution and, subsequently be reduced to metal with the reducing properties of the polymer [40].

As expected from XRD results, silver nanoparticles were observed on charged EPS by

TEM. Figure 5 presents TEM pictures for the EPS M3 after biosorption. Nanoparticles display different shapes such as spheres or triangles with different sizes. Some of them show a core-shell structure. We note that the nanoparticles are well dispersed and form a colloidal solution. Indeed, EPS is known to stabilize the silver nanoparticles by preventing the aggregation/flocculation processes [41]. Similar results were observed for all EPS

4. Conclusion

In this study, XRD, XPS, FTIR and TEM were used to study mechanisms involved in silver sorption by four bacterial EPS (M1, M2, M3, M4) differing in their native chemical composition. For EPS M2, M3 and M4, results clearly showed the involvement of hydroxyl and carboxyl functional groups in trapping silver ions. Concerning EPS M2 and M4, for which it had been demonstrated fewer biosorption capacities, change of EPS composition was observed concomitantly to silver sorption, with a relative increase of carboxylate content compared to hydroxyl groups. This behaviour was correlated to the formation of silver oxides nanoparticles, though it is unclear whether these particles formed before, during, or after the sorption of Ag^{+} to the EPS. After biosorption, the presence of these nanoparticles might impact the physical or chemical treatment needed to recover silver from EPS. Further studies are needed to explore this possible impact. Moreover, original result of this work is the evidence that sulfates groups of EPS M1 play a major role in sorption process of silver.

Acknowledgements

The authors acknowledge G. Sinquin and P. Elies from for TEM measurements. We also thank C. Liorzou from Pôle Spectrométrie Océan, IUEM for metal analysis on ICP AES.

References

[1] L. Lanceleur, L'argent: sources, transfert et bioaccumulation: cas du système fluvio-estuarien girondin, 2011.

[2] R. Eisler, Silver Hazards to Fish, Wildlife, and Invertebrates: A Synoptic Review. DTIC Document, 1996.

[3] N.S. Fisher, W.X. Wang, Trophic transfer of silver to marine herbivores: A review of recent studies, Environmental toxicology and chemistry 17 (1998) 562-571.

[4] H.T. Ratte, Bioaccumulation and toxicity of silver compounds: A review, Environmental Toxicology and Chemistry 18 (1999) 89-108.

[5] H.C. Tao, Z.Y. Gao, H. Ding, N. Xu, W.M. Wu, Recovery of silver from silver (I)-containing solutions in bioelectrochemical reactors, Bioresource technology 111 (2012) 92-97.

[6] I. Rivera, G. Juàrez, F. Patino, I.A. Reyes, A. Roca, M.I. Reyes, Silver precipitation using sodium dithionite in cyanide media, J. Mex. Chem. Soc, 56 (2012) 156-162.

[7] N. Acarkan, G. Bulut, A. Gül, O. Kangal, F. Karakas, O. Kökkiliç, G., Onal, The effect of collector's type on gold and silver flotation in a complex ore, Separation Science and Technology 46 (2010) 283-289.

[8] S. Coruh, G., Senel, O.N. Ergun, A comparison of the properties of natural clinoptilolites and their ion-exchange capacities for silver removal, Journal of hazardous materials 180, (2010) 486-492.

[9] M.A. Abd El-Ghaffar, M.H. Mohamed, K.Z., Elwakeel, Adsorption of silver (I) on synthetic chelating polymer derived from 3-amino-1, 2, 4-triazole-5-thiol and glutaraldehyde. Chemical engineering journal 151 (2009) 30-38.

[10] K.Z. Elwakeel, G.O. El-Sayed, R.S., Darweesh, Fast and selective removal of Silver (I) from aqueous media by modified chitosan resins, International Journal of Mineral Processing 120 (2013) 26-34.

[11] A.V. Pethkar, S.K. Kulkarni, K.M. Paknikar, Comparative studies on metal biosorption by two strains of *Cladosporium cladosporioides*, Bioresource technology, 80, (2001) 211-215.

[12] M.L. Merroun, N.B. Omar, E. Alonso, J.M. Arias, M.T. Gonzalez-Munoz, Silver sorption to Myxococcus xanthus biomass, Geomicrobiology Journal 18 (2001) 183-192.

[13] M. Gurung, B.B. Adhikari, H. Kawakita, K. Ohto, K. Inoue, S. Alam, Recovery of gold and silver from spent mobile phones by means of acidothiourea leaching followed by adsorption using biosorbent prepared from persimmon tannin, Hydrometallurgy 133 (2013) 84-93.

[14] J.L. Geddie, I.W. Sutherland, Uptake of metals by bacterial polysaccharides, J. Appl. Microbiol. 74 (1993) 467-472.

[15] M. Loaëc, R. Olier, J. Guezennec, Uptake of lead, cadmium and zinc by a novel bacterial exopolysaccharide, Water Res. 31 (1997) 1171-1179.

[16] M. Loaëc, R. Olier, J. Guezennec, Chelating properties of bacterial exopolysaccharides from deep-sea hydrothermal vents, Carbohyd. Polym. 35 (1998) 65-70.

[17] S. Comte, G. Guibaud, M. Baudu, Biosorption properties of extracellular polymeric substances (EPS) resulting from activated sludge according to their type: Soluble or bound, Process Biochem. 41 (2006) 815-823.

[18] X. Moppert, T. Le Costaouec, G. Raguenes, A. Courtois, C. Simon-Colin, P. Crassous, B. Costa, J. Guezennec, Investigations into the uptake of copper, iron and selenium by a highly sulphated bacterial exopolysaccharide isolated from microbial mats, J. Ind. Microbiol. Biot. 36 (2009) 599-604.
[19] M. Deschatre, F. Ghillebaert, J. Guezennec, C. Simon-Colin, Sorption of Copper (II) and Silver (I) by Four Bacterial Exopolysaccharides, Applied biochemistry and biotechnology 171 (2013) 1313-1327.
[20] G. Raguènes, X. Moppert, L. Richert, J. Ratiskol, C. Payri, B. Costa, et al. A novel exopolymer-producing bacterium, *Paracoccus zeaxanthinifaciens* subsp. *payriae*, isolated from a kopara mat located in Rangiroa, an atoll of French Polynesia, Current Microbiology, 49 (2004) 145–151.
[21] M. Salou, B. Lescop, S. Rioual, A. Lebon, J. BenYoussef, B. Rouvellou, Initial oxidation of polycrystalline Permalloy surface, Surface Science, 602 (2008) 2901-2906.
[22] B. Volesky, Biosorption and me, Water Res. 41 (2007) 4017-4029.
[23] P. Fardim, N. Duràn, Modification of fibre surfaces during pulping and refining as analysed by SEM, XPS and ToF-SIMS, Colloids and Surfaces A: Physicochemical and Engineering Aspects 223 (2003) 263-276.
[24] L. Fras, L.S. Johansson, P. Stenius, J. Laine, K. Stana-Kleinschek, V. Ribitsch, Analysis of the oxidation of cellulose fibres by titration and XPS, Colloids and Surfaces A: Physicochemical and Engineering Aspects 260 (2005) 101-108.
[25] Y. Liu, Z. Yu, S. Zhou, L. Wu, Self-assembled monolayers on magnesium alloy surfaces from carboxylate ions, Applied Surf. Sci. 252 (2006) 3818-3827.
[26] A. Omoike, J. Chorover, Spectroscopic Study of Extracellular Polymeric Substances from Bacillus s ubtilis: Aqueous Chemistry and Adsorption Effects, Biomacromolecules 5 (2004) 1219-1230.
[27] H.S. Shin, H.C. Choi, Y. Jung, S.B. Kim, H.J. Song, H.J. Shin, Chemical and size effects of nanocomposites of silver and polyvinyl pyrrolidone determined by X-ray photoemission spectroscopy. Chem. Phys. Lett. 383 (2004) 418-422.
[28] K.J. Lee, Y.I. Lee, I.K. Shim, J., Joung, Y.S. Oh, Direct synthesis and bonding origins of monolayer-protected silver nanocrystals from silver nitrate through in situ ligand exchange, Journal of colloid and interface science 304 (2006) 92-97.
[29] T.Y. Dong, W.T. Chen, C.W. Wang, C.P. Chen, C.N. Chen, M.C. Lin, J.M. Song, I.G. Chen, T.H. Kao, One-step synthesis of uniform silver nanoparticles capped by saturated decanoate: direct spray printing ink to form metallic silver films, Phys. Chem. Chem. Phys. 11 (2009) 6269-6275.
[30] D. Zemlyanov, G. Weinberg, U. Wild, R. Schlägl, Formation of a liquid film of $AgNO_3$ on a silver surface, Catalysis Lett. 64 (2000) 113-118.
[31] Z. Lin, C. Zhou, J. Wu, J. Zhou, L. Wang, A further insight into the mechanism of Ag^+ biosorption by *Lactobacillus sp.* strain A09, Spectrochimica Acta Part A: Molecular and Biomolecular Spectroscopy 61 (2005) 1195-1200.
[32] S.K. Papageorgiou, E.P. Kouvelos, E.P. Favvas, A.A. Sapalidis, G.E. Romanos, F.K. Katsaros, Metal carboxylate interactions in metal alginate complexes studied with FTIR spectroscopy, Carbohydrate research 345 (2010) 469-473.
[33] M. Kacurakova, P. Capek, V. Sasinkova, N. Wellner, A. Ebringerova, FTIR study of plant cell wall model compounds: pectic polysaccharides and hemicelluloses, Carbohydrate Polymers 43 (2000) 195-203.

[34] P. Simmons, I. Singleton, A method to increase silver biosorption by an industrial strain of Saccharomyces cerevisiae, Applied microbiology and biotechnology 45 (1996) 278-285.
[35] M.A.S. Sadjadi, B. Sadeghi, M. Meskinfam, K. Zare, J. Azizian, Synthesis and characterization of Ag/PVA nanorods by chemical reduction method, Physica E: Low-dimensional Systems and Nanostructures 40 (2008) 3183-3186.
[36] S. Pal, G. De, Reversible transformations of silver oxide and metallic silver nanoparticles inside SiO_2 films, Materials Research Bulletin 44 (2009) 355-359.
[37] A. Ahmad, P. Mukherjee, S. Senapati, D. Mandal, M.I. Khan, R. Kumar, M. Sastry, Extracellular biosynthesis of silver nanoparticles using the fungus *Fusarium oxysporum*, Colloids and Surfaces B: Biointerfaces 28 (2003) 313-318.
[38] A. Panacek, L. Kvitek, R. Prucek, M. Kolar, R. Vecerova, N. Pizurova, V.K. Sharma, T.J. Nevecna, R. Zboril, Silver colloid nanoparticles: synthesis, characterization, and their antibacterial activity, J. Phys. Chem. B 110 (2006) 16248-16253.
[39] K.S. Chou, C.Y. Ren, Synthesis of nanosized silver particles by chemical reduction method, Materials Chemistry and Physics 64 (2000) 241-246.
[40] H.H. Nersisyan, J.H. Lee, H.T. Son, C.W. Won, D.Y. Maeng, A new and effective chemical reduction method for preparation of nanosized silver powder and colloid dispersion, Materials Research Bulletin 38 (2003) 949-956.
[41] S.S. Khan, A. Mukherjee, N. Chandrasekaran, Impact of exopolysaccharides on the stability of silver nanoparticles in water, Water research 45 (2011) 5184-5190.

Figures

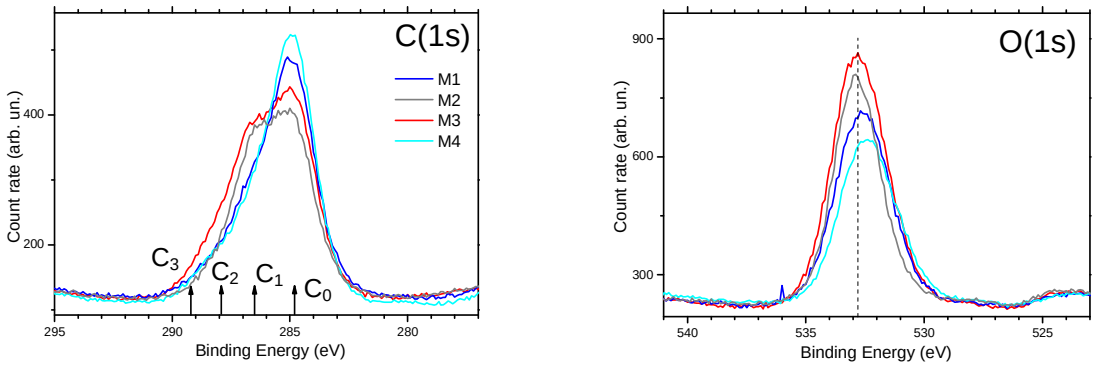

Fig. 1.a) C(1s) and b) O(1s) XPS spectra of EPS before biosorption of silver.

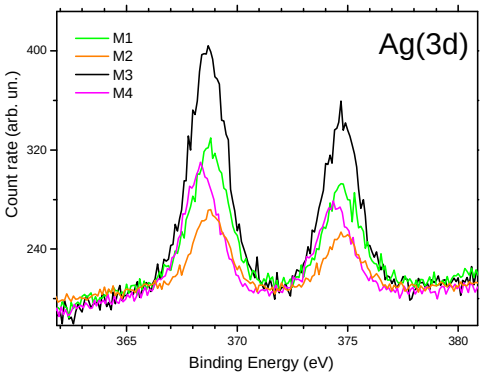

Fig. 2. Ag (3d) spectra of EPS

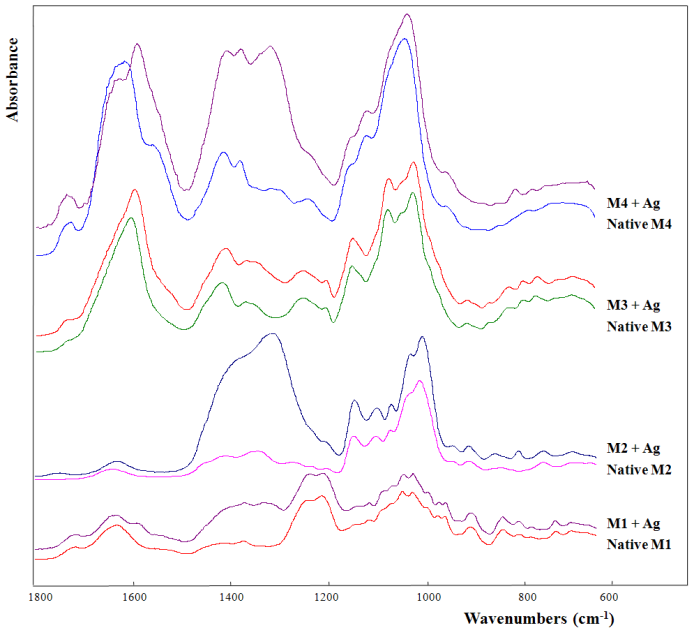

Fig. 3. FTIR spectra of EPS before and after biosorption.

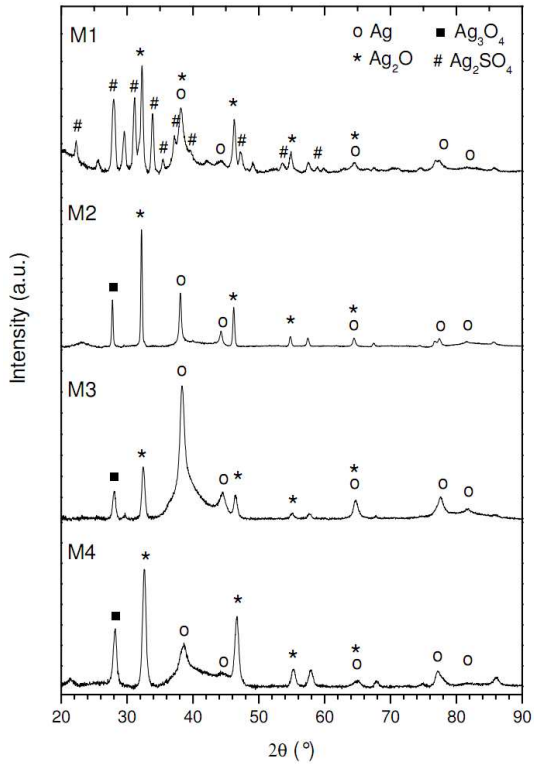

Fig. 4. XRD patterns of M1 – M4 EPS after Ag biosorption

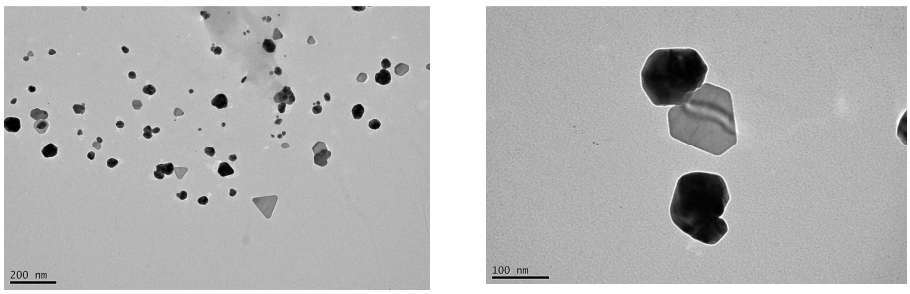

Fig. 5. TEM images of the EPS M3 after Ag biosorption.